

EVIDENCE FOR SPIN AND ENERGY EXTRACTION IN A GALACTIC BLACK HOLE CANDIDATE: THE *XMM-NEWTON*/EPIC-PN SPECTRUM OF XTE J1650–500

J. M. MILLER¹, A. C. FABIAN², R. WIJNANDS^{1,3}, C. S. REYNOLDS⁴, M. EHLE⁵, M. J. FREYBERG⁶,
M. VAN DER KLIS⁷, W. H. G. LEWIN¹, C. SANCHEZ-FERNANDEZ⁸, A. J. CASTRO-TIRADO⁹

Draft version October 30, 2018

ABSTRACT

We observed the Galactic black hole candidate XTE J1650–500 early in its Fall, 2001 outburst with the *XMM-Newton* European Photon Imaging pn Camera (EPIC-pn). The observed spectrum is consistent with the source having been in the “very high” state. We find a broad, skewed Fe K α emission line which suggests that the primary in this system may be a Kerr black hole, and which indicates a steep disk emissivity profile that is hard to explain in terms of a standard accretion disk model. These results are quantitatively and qualitatively similar to those from an *XMM-Newton* observation of the Seyfert galaxy MCG–6-30-15. The steep emissivity in MCG–6-30-15 may be explained by the extraction and dissipation of rotational energy from a black hole with nearly-maximal angular momentum or material in the plunging region via magnetic connections to the inner accretion disk. If this process is at work in both sources, an exotic but fundamental general relativistic prediction may be confirmed across a factor of 10⁶ in black hole mass. We discuss these results in terms of the accretion flow geometry in stellar-mass black holes, and the variety of enigmatic phenomena often observed in the very high state.

Subject headings: physical data and processes: black hole physics – X-rays: stars – stars: binaries (XTE J1650–500)

1. INTRODUCTION

The accretion flow geometry in stellar-mass black holes may change considerably with the mass accretion rate (\dot{m}). Characteristic periods of correlated intensity, energy spectral hardness, and fast variability in the X-ray band are identified as “states” (for a review, see Tanaka & Lewin 1995; see also Homan et al. 2001). These states are observed in all stellar-mass black holes, and are thought to be driven primarily by changes in \dot{m} .

Of five common states, the “very high” state is perhaps the least-understood. Often the first state observed in a transient outburst and usually very luminous, a variety of phenomena are observed that indicate a unique inner accretion flow environment. Fast quasi-periodic oscillations (QPOs; 30–450 Hz) — if tied to the Keplerian frequency of the inner accretion disk — indicate accretion disks which extend close to the marginally stable circular orbit for a Schwarzschild black hole, and may even indicate black hole spin (e. g., Strohmayer 2001, Miller et al. 2001a). Discrete jet ejections are sometimes observed in the radio band with velocities that approach c (for a review, see Fender 2001). The X-ray energy spectra observed in the very high state are a mix of thermal and non-thermal components. The spectra suggest a disk which may extend close to the black hole, and a corona (the assumed non-thermal source) which irradiates the disk and produces a “reflection” spectrum (George & Fabian 1991; see also Gierlinski et al. 1999).

With adequate spectral resolution, Fe K α line profiles may

provide effective tools for constraining the nature of accretion flows (e. g. Miller et al. 2002) in stellar-mass black holes. Such profiles have been used to infer black hole spin and rotational energy extraction via magnetic fields in active galactic nuclei (AGNs; Iwasawa et al. 1996, Wilms et al. 2001). Evidence for spin, based on Fe K α line profiles, has also been reported in stellar-mass black holes, but with gas proportional counters offering lower resolution and inhibiting stronger conclusions (Balucinska-Church & Church 2000, Miller et al. 2001b, Campana et al. 2002). The high effective area of *XMM-Newton* and short frame times available with the EPIC-pn camera are well-suited to capturing high resolution spectra of bright sources.

We were granted a target-of-opportunity observation to study the Galactic black hole candidate XTE J1650–500 (Remillard 2001) early in its Fall, 2001 outburst. Although a neutron star primary can only be ruled-out by optical radial velocity measurements, there is strong evidence in X-rays that XTE J1650–500 harbors a black hole. Based on the spectrum we obtained with *XMM-Newton* and timing properties (Wijnands, Miller, & Lewin 2001), we observed XTE J1650–500 in the very high state — the first pile-up-free CCD spectrum of a stellar-mass black hole in this state. Herein, we report the detection of a broad Fe K α line. We discuss the implications of this line for the accretion flow geometry in this source, and explore connections to the recent *XMM-Newton* observation of the Seyfert-I AGN MCG–6-30-15 (Wilms et al. 2001).

¹Center for Space Research and Department of Physics, Massachusetts Institute of Technology, 70 Vassar Street, Cambridge, MA 02139–4307; jmm@space.mit.edu

²Institute of Astronomy, University of Cambridge, Madingley Road, Cambridge CB3 0HA, UK

³*Chandra* Fellow

⁴Department of Astronomy, University of Maryland, College Park, MD, 20742

⁵*XMM-Newton* SOC, Villafranca Satellite Tracking Station, PO Box 50727, 28080, Madrid, ES & Research and Scientific Support Dept. of ESA, Noordwijk, NL

⁶Max-Planck-Institut für extraterrestrische Physik, Postfach 1312, 85741 Garching, DE

⁷Astronomical Institute “Anton Pannekoek,” University of Amsterdam, and Center for High Energy Astrophysics, Kruislaan 403, 1098 SJ, Amsterdam, NL

⁸Laboratorio de Astrofísica Espacial y Física Fundamental (LAEFF-INTA), PO Box 50727, E-28080, Madrid, ES

⁹Instituto de Astrofísica de Andalucía (IAA-CSIC), P. O. Box 03004, E18080–Granada, ES & LAEFF-INTA, Madrid, ES

2. OBSERVATION AND DATA REDUCTION

We observed XTE J1650–500 with *XMM-Newton* on 13 September, 2001, from 15:45:25–21:41:04 (UT) for a total exposure of 21.4 ks. We did not operate the EPIC-MOS2 camera or the Optical Monitor to preserve telemetry. The EPIC-MOS1 camera was operated in timing mode but suffered a full scientific buffer nearly continuously due to the high flux. Full spectral results from the Reflection Grating Spectrometer (RGS, 0.33–2.5 keV) will be reported in a separate paper. To prevent photon pile-up, the EPIC-pn camera was operated in “burst” mode with the “thin” optical filter in place (for more information on the pn camera, see Stüder et al. 2001). Only one CCD of the pn camera is active in burst mode, and spatial information is only recorded in one dimension. Burst mode has a time resolution of 7 μ s, but a duty cycle of approximately 3%.

We extracted source counts using a box region centered on the source position (with X and Y half-widths of 1694 and 28, respectively, in DET units). Two background regions adjacent to the source position were selected. Single and double events were included for analysis. Standard pn filtering was accomplished with the procedure XMMEA_EP, assuming a source position of $16^{\circ}50'01.0''$, $-49^{\circ}57'45''$ (Castro-Tirado et al. 2001; Groot et al. 2001). We measured a source count rate of 2557.0 ± 1.9 counts s^{-1} , and a background count rate of 151.5 ± 0.5 counts s^{-1} . Calibrated event lists were custom-made at MPE using SAS–5.3 α . The source and background spectra were created with SAS–5.2.0. Spectra were grouped based both on a requirement for counts per channel (20) and on the maximum number of spectral channels sampling the pn energy resolution (3).

This is the first spectral analysis to be reported from an observation which employed burst mode. Despite the peculiarities of this mode, the instrumental effective area and the energy response, and charge transfer inefficiency (CTI) correction do not differ from more standard modes (Kirsch et al. 2002). Therefore, “full frame” mode response matrices were created to model the instrument response using SAS–5.2.0.

The spectral fits reported herein were made using XSPEC version 11.1.0 (Arnaud 1996). Quoted errors correspond to $\Delta \chi^2 = 1.0$. Below 0.5 keV and above 10.0 keV, deviations were seen in the residuals regardless of the spectral model used. We therefore restricted our analysis to the 0.5–10.0 keV band. We note a feature at 2.34 keV which appears as an emission line. The detector effective area changes sharply at this energy and the line is well-fit by a zero-width Gaussian, suggesting that the feature is instrumental.

3. ANALYSIS AND RESULTS

In examining the EPIC-pn and RGS data of XTE J1650–500, we find oxygen to be $13_{-5}^{+1}\%$ under-abundant, neon to be $16_{-6}^{+8}\%$ over-abundant, and iron to be $45 \pm 5\%$ under-abundant relative to solar values along this line of sight (assuming abundances as measured by Anders & Grevesse 1989). The RGS spectrum reveals that the oxygen edge location is more consistent with 0.536 keV than the expected 0.532 keV; this has also been noted in fits to Chandra data of Cygnus X-1 (Schulz et al. 2001, Miller et al. 2002). We therefore fixed the oxygen edge to be at 0.536 keV in all fits. All other elements are found to have abundances consistent with solar values.

Absorption in the ISM was modeled using the “vphabs” model in XSPEC (with the abundance of oxygen set to zero,

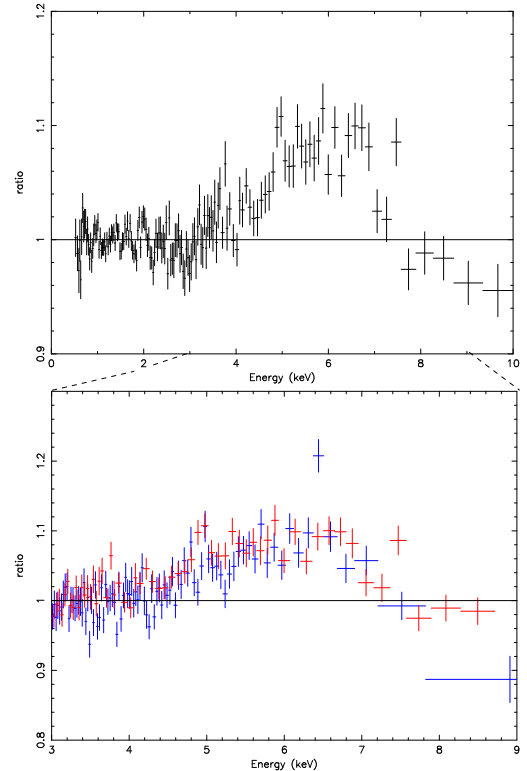


FIG. 1.— Above: The data/model ratio for a model consisting of multicolor disk blackbody and power-law components, modified by photoelectric absorption. (We have suppressed a feature at 2.34 keV; the data is fit between 0.5–10.0 keV) Below: The data/model ratio of XTE J1650–500 (in red) and that for a 30 ksec observation of Cygnus X-1 with the *Chandra* High Energy Transmission Grating Spectrometer (in blue), shown in greater detail than above. In all ratios shown above, the 4.0–7.0 keV band was ignored in fitting the model. The ratios have been rebinned for visual clarity. In both, a majority of the line profile lies below 6.40 keV, the $K\alpha$ line energy for neutral Fe.

and an additional edge to model the oxygen absorption at 0.536 keV). We measure an effective neutral hydrogen column density of $N_H = 7.8 \pm 0.2 \times 10^{21}$ atoms cm^{-2} .

Fits with the standard multicolor accretion disk black body (hereafter, MCD; Mitusda et al. 1984) plus power-law model to the 0.5–10.0 keV spectrum were statistically unacceptable ($\chi^2 = 513.4$ for 233 d.o.f.). The data/model ratio for this model is shown in Figure 1. The emission line profile in this data/model ratio is similar to that observed in Cygnus X-1 with the *Chandra* High Energy Transmission Grating Spectrometer (Miller et al. 2002), and similar to line profiles seen in some AGNs with *ASCA* (see, e. g., Iwasawa et al. 1996; Weaver, Gelbord, & Yaqoob 2001).

Gaussian emission line and smeared edge (see Ebisawa et al. 1994) components were added to the model. The addition of these components improved the fit significantly ($\chi^2 = 314.8$ for 225 d.o.f.). Using this model, we measure an inner disk color temperature of $kT = 0.322 \pm 0.004$ keV, and an MCD normalization of $3.9_{-1.3}^{+0.3} \times 10^4$. The measured power-law index is $\Gamma = 2.09_{-0.09}^{+0.03}$, the normalization of this component is measured to be 3.1 ± 0.2 ph $cm^{-2} s^{-1} keV^{-1}$ at 1 keV. The 0.5–10.0 keV flux of the MCD component is $0.36_{-0.12}^{+0.03} \times 10^{-8}$ erg $cm^{-2} s^{-1}$, and that for the power-law component is $1.17 \pm 0.08 \times 10^{-8}$ erg $cm^{-2} s^{-1}$.

The best-fit Gaussian indicates a broad line, shifted from the neutral Fe $K\alpha$ line energy of 6.40 keV: $E = 5.3_{-0.3}^{+0.1}$ keV, $FWHM = 3.2_{-0.6}^{+0.8}$ keV, and $W = 250 \pm 50$ eV. The edge is measured to be at $E = 6.8 \pm 0.3$ keV, with a depth of $\tau = 0.5 \pm 0.1$. However, significant residuals remain in the Fe $K\alpha$ line region with this fit, due in part to the non-Gaussian nature of

the line profile (see Figure 1). Moreover, on a broader energy range (one that includes the 20–30 keV “Compton hump” seen in many sources), a reflection model is often required to fit the spectra of stellar-mass black holes (see, e.g., Gierlinski et al. 1999). Broad Gaussian and smeared edge components are merely an approximation to a full reflection model in the 0.5–10.0 keV band. Therefore, we now focus on the results of fitting more sophisticated, physically-motivated reflection models. These replace the hard power-law, Gaussian, and smeared edge components discussed above.

Anticipating a highly-ionized accretion disk, we made fits with the “constant density ionized disk” reflection model (hereafter, CDID; Ross, Fabian, & Young 1999). This model measures the relative strengths of the directly-observed and reflected flux, the accretion disk ionization parameter ($\xi = L_X/nR^2$, where L_X is the X-ray luminosity, n is the hydrogen number density, and R is radius), and the photon index of the illuminating power-law flux. Fe $K\alpha$ line emission and line broadening due to Comptonization in an ionized disk surface layer are included in this model.

The fit obtained with this model is shown in the top panel of Figure 2. The photon index of the irradiating power law is measured to be $\Gamma = 2.08^{+0.02}_{-0.04}$. The ionization parameter is high: $\xi = 1.3^{+0.7}_{-0.1} \times 10^4$ erg cm s $^{-1}$, and the relative strength of reflected flux is measured to be $f = 0.5^{+0.7}_{-0.1}$ (where $F_{total} = F_{direct} + f \times F_{refl}$). While the shape of the Fe K edge is reproduced by this model, the width and shape of the Fe $K\alpha$ line is not, and a statistically-poor fit is obtained ($\chi^2 = 399.7$ for 231 d.o.f.). The ionization parameter obtained with this model corresponds to a mixture of helium-like and hydrogenic ion species of Fe (Kallman and McCray 1982).

As Doppler shifts and general relativistic smearing may be expected for lines produced in an accretion disk close to the black hole, we next made fits after convolving (or, “blurring”) the CDID model with the line element expected near a Kerr black hole. We assumed an inner disk radius of $1.24 R_g$, an outer line production radius of $400 R_g$, and an inclination of $i = 45^\circ$ (in fits with this and other models, intermediate inclinations were marginally preferred in terms of χ^2). With this blurred model, we obtained parameter constraints which differed marginally from the previous fit: $\xi = 2.5^{+5.5}_{-0.1} \times 10^4$ erg cm s $^{-1}$, $f = 0.6^{+0.6}_{-0.1}$, and $\Gamma = 1.96^{+0.04}_{-0.06}$. The shape and strength of the Fe $K\alpha$ line are not fit adequately; the fit is slightly worse than the un-blurred model ($\chi^2 = 407.8$, 231 d.o.f.).

Finally, we constructed a model which allows the Fe $K\alpha$ line and reflection components to be treated separately. We fit the line with the “Laor” line model (Laor 1991), and the power-law and reflection continuum (minus the line) with the “pexriv” model (Magdziarz & Zdziarski 1995). With pexriv, $f = 1$ corresponds to a disk which intercepts half of the incident power-law flux. It should be noted that this model was also used by Wilms et al. (2001) in fits to the *XMM-Newton*/EPIC spectrum of the Seyfert galaxy MCG–6–30–15, allowing for a direct comparison. For the Laor line, we initially fixed the inner disk edge at $1.24 R_g$, the outer line production region at $400 R_g$, and the inclination at $i = 45^\circ$. The line energy, emissivity profile ($\epsilon \sim r^{-\beta}$; we fit for β), and intensity were allowed to vary. The MCD and pexriv reflection components were blurred as before.

We found that the data could not simultaneously constrain f , ξ , and the disk surface temperature with pexriv (an additional

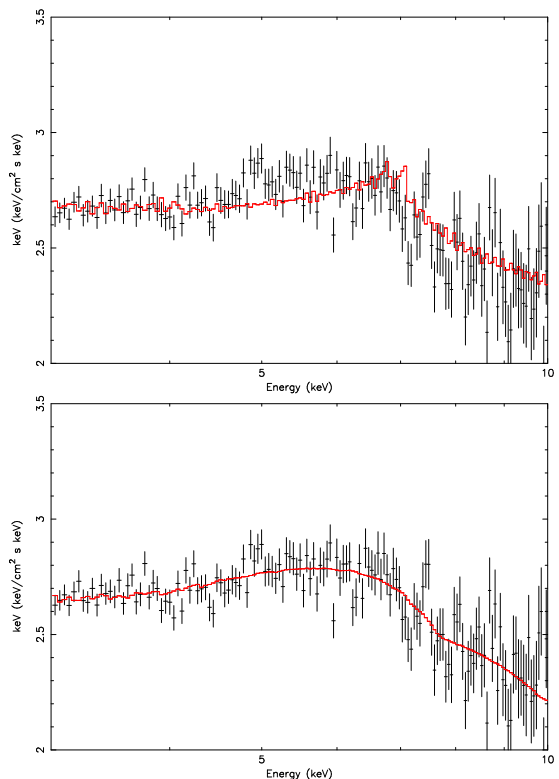


FIG. 2.— *Top*: the spectrum of XTE J1650–500 fit with a model for disk reflection (shown in red is the “constant density ionized disk” model; Ross, Fabian, & Young 1999). Clearly, the line profile is broader than is predicted with this model, indicating significant Doppler shifts and/or general relativistic skewing are required to describe the line profile. *Bottom*: The spectrum fit with the “Laor” model for line emission near a Kerr black hole (Laor 1991), and the “pexriv” reflection model (Magdziarz & Zdziarski 1995).

parameter for this model). We therefore fixed the ionization parameter at $\xi = 2.0 \times 10^4$ erg cm s $^{-1}$, and the disk surface temperature at $kT = 1.3$ keV (as per Ross, Fabian, & Young 1999 in fits to Cygnus X-1, wherein a similarly low MCD disk temperature but similarly high values of ξ are reported).

The fit obtained with this model is shown in the bottom panel of Figure 2. Statistically, this model represents a significant improvement ($\chi^2 = 319.9$ for 229 d.o.f.). A power-law index of $\Gamma = 2.04^{+0.03}_{-0.02}$ is obtained. We measure the Fe $K\alpha$ line to be centered at $E = 6.8^{+0.2}_{-0.1}$ keV, likely due to a blend of Fe XXV and Fe XXVI (helium-like and hydrogenic Fe) and consistent with the high ionization parameters previously measured. The line is strong, with an equivalent width of $W = 350^{+60}_{-40}$ eV and a flux of $2.2 \pm 0.3 \times 10^{-10}$ erg cm $^{-2}$ s $^{-1}$ ($3.2 \pm 0.4 \times 10^{-2}$ ph cm $^{-2}$ s $^{-1}$). When the inner disk edge is allowed to vary, an inner radius of $1.24 R_g$ (the limit of the Laor model, corresponding to $a = 0.998$) is preferred over an inner radius of $6.0 R_g$ (the marginally stable circular orbit around a Schwarzschild black hole) at the 6σ level of confidence. A steep emissivity is suggested via the Laor line model: $\beta = 5.4 \pm 0.5$. This emissivity is preferred over that for a standard accretion disk ($\beta = 3.0$) at the 5.6σ level of confidence. The pexriv reflection “fraction” is $f = 0.6^{+0.3}_{-0.1}$. This is consistent with the reflection fractions measured in the high state of Cygnus X-1 (Gierlinski et al. 1999), wherein the disk may extend to the marginally stable circular orbit.

It is not likely that these results can be explained in terms of an anomalous Fe abundance. Allowing β and A_{Fe} (in pexriv) to vary, the abundance is poorly constrained: $A_{Fe} = 1.0^{+0.5}_{-0.7}$, and the emissivity drops only slightly to $\beta = 5.0$. Fixing the emissivity at $\beta = 3.0$ and allowing the Fe abundance to vary yields

a significantly worse fit ($\chi^2 = 353.1$ for 229 d.o.f.) and Fe must be more than 30 times over-abundant. We note that the line strength and reflection fraction in our final fit are not strictly congruent, and that $f = 0.6_{-0.1}^{+0.3}$ is below the reflection fraction measured in MCG–6–30–15 ($f = 1.5–2.0$, Wilms et al. 2001) using a similar model. If we fix the $f = 1.5$ in our final model, χ^2 increases only slightly ($\chi^2 = 324.9$ for 230 d.o.f.), and the other fit parameters only change within their 1σ confidence intervals. Thus, more congruent values of f are allowed by the data.

The high χ^2 value associated with our final model could be due to unmodeled narrow spectral features, approximations in the model, and calibration issues. We note a feature at approximately 7.0 keV, which may be a narrow edge due to neutral Fe or an Fe XXVI absorption line. Alternatively, there may be an Fe K β emission line near 7.4 keV due to ionized Fe species, which is superimposed upon the broader smeared edge fit by the reflection models. There is also weak evidence for a narrow absorption edge feature near 9.3 keV, consistent with Fe XXVI. Modeling these features and the addition of 0.5% systematic errors below 1 keV are sufficient to make the fit acceptable.

4. DISCUSSION

We have observed a broad Fe K α line profile in the *XMM-Newton*/EPIC-pn spectrum of the Galactic black hole candidate XTE J1650–500 in the very high state. A comparison with the broad line profile observed with *Chandra* in Cygnus X-1 is shown in Figure 1. That such profiles are observed in very different systems, strongly suggests that broad Fe K α lines in stellar-mass black holes stem from a common process. Like the broad lines observed in some Seyfert AGNs, these lines are likely produced by irradiation of the inner disk.

The Fe K α line we have observed in XTE J1650–500 suggests a Kerr black hole with near-maximal angular momentum ($a = 0.998$). The accretion disk emissivity profile measured with the Laor line model is inconsistent with the energy dissipation expected for standard disks. These results are very similar to those reported by Wilms et al. (2001) using the same line and reflection models for the broad Fe K α line observed in an *XMM-Newton*/EPIC-pn spectrum of the Seyfert galaxy MCG–6–30–15 ($E = 6.97_{-0.10}$ keV, $W \sim 300–400$ eV, $f = 1.5–2$, $\beta \sim 4.3–5.0$). Those authors suggest that rotational energy

extraction from the spinning black hole (Blandford & Znajek 1977) or material in the plunging region (Agol & Krolik 2000) may infuse the inner accretion disk with extra energy via magnetic connections, creating the steep emissivity profile indicated by the Fe K α line. It is possible that rotational energy extraction may be at work in XTE J1650–500 as well. If so, a fundamental general relativistic prediction may be confirmed across a factor of roughly 10^6 in black hole mass.

This observation suggests a connection between the accretion geometry of stellar-mass black holes in the very high state, and that inferred in some Seyfert galaxies. This is an important step towards understanding the nature of the very high state, and the variety of exotic phenomena observed in this state. The Blandford–Znajek process is also often invoked as a means of launching jets (Blandford 2001a, 2001b; see also Fender 2001). That we have found an emissivity which might be explained by magnetic connections to the black hole or to matter in the plunging region in the very high state of XTE J1650–500 (detected at 7.5 mJy at 0.8 GHz with MOST in this state with a spectrum indicative of jets; S. Tingay, priv. comm.), suggests that the discrete radio ejections observed in some sources in this state (see Fender 2001) may be driven by rotational energy extraction.

Martocchia, Matt, & Karas (2002) have shown that a “lamp-post” reflection model may explain the steep disk emissivity implied in fits to the Fe K α line in MCG–6–30–15. This model assumes a source of power-law flux which illuminates the accretion disk from a location directly above the black hole. To explain $\beta \sim 4$, this model requires $f \sim 4$ — well above the values we measure. Therefore, the lamp-post model may not adequately describe the accretion geometry of XTE J1650–500.

5. ACKNOWLEDGMENTS

We wish to thank *XMM-Newton* project scientist Fred Jansen for executing our TOO request. RW was supported by NASA through Chandra fellowship grants PF9-10010, which is operated by the Smithsonian Astrophysical Observatory for NASA under contract NAS8–39073. This work is based on observations obtained with *XMM-Newton*, an ESA science mission with instruments and contributions directly funded by ESA Member States and the USA (NASA).

REFERENCES

- Agol, E., & Krolik, J. H., 2000, *ApJ*, 528, 161
 Anders, E., & Grevesse, N., 1989, *GeoCoA*, 53, 197
 Arnaud, K. A., 1996, *Astronomical Data Analysis Software and Systems V*, eds. Jacoby G. and Barnes J., p17, ASP Conf. Series volume 101
 Balucinska-Church, M., & Church, M. J., 2000, *MNRAS*, 312L, 55
 Blandford, R. D., 2001a, to appear in “Particles and Fields in Radio Galaxies,” ASP Conference Series, eds. R. A. Laing and K. M. Blundell
 Blandford, R. D., 2001b, *Prog. of Th. Phys. Supplement Series*, in press
 Blandford, R. D., & Znajek, R. L., 1977, *MNRAS*, 179, 433
 Campana, S., et al., 2002, *A & A*, in press, astro-ph/0112485
 Castro-Tirado, A. J., et al., 2001, *IAU Circ.* 7707
 Ebisawa, K., et al., 1994, *PASJ*, 46, 375
 Fender, R. P., 2001, to appear in “Relativistic Flows in Astrophysics,” Springer Verlag Lecture Notes in Physics, eds. A. W. Guthmann et al.
 George, I. M., & Fabian, A. C., 1991, *MNRAS*, 249, 352
 Gierlinski, M., Zdziarski, A. A., Poutanen, J., Coppi, P. S., Ebisawa, K., and Johnson, W. N., 1999, *MNRAS* 309, 496
 Groot, P., Tingay, S., Udalski, A., & Miller, J. M., 2001, *IAU Circ.* 7708
 Homan, J., et al., 2001, *ApJ*, 132S, 377
 Iwasawa, K., Fabian, A. C., Young, A. J., Inoue, H., and Matsumoto, C., 1999, *MNRAS*, 306L, 19
 Kallman, T. R. and McCray, R., 1982, *ApJS*, 50, 263
 Kirsch, M., Kendziorra, E., Freyberg, M. J., & Edele, A., 2002, in “New Visions on the X-ray Universe in the XMM-Newton and Chandra Era”, Noordwijk, ESA SP-488
 Laor, A., 1991, *ApJ*, 376, 90
 Magdziarz, P., & Zdziarski, A. A., 1995, *MNRAS*, 273, 837
 Martocchia, A., Matt, G., & Karas, V., 2002, *A & A*, subm., astro-ph/0201192
 Miller, J. M., et al., 2001a, *ApJ*, 563, 928
 Miller, J. M., et al., 2001b, *ApJ*, 546, 1055
 Miller, J. M., et al., 2002, *ApJ*, subm., astro-ph/0202083
 Mitsuda, K., et al., 1984, *PASJ*, 36, 741
 Remillard, R., 2001, *IAU Circ.* 7707
 Ross, R. R., Fabian, A. C., & Young, A. J., 1999, *MNRAS*, 306, 461
 Schulz, N. S., et al., 2001, *ApJ*, in press
 Strohmayer, T. E., 2001, *ApJ*, 552L, 49
 Stüder, L., et al., 2001, *A & A*, 365, L18
 Tanaka, Y., and Lewin, W. H. G., 1995, *X-ray Binaries*, ed. W. H. G. Lewin et al. (Cambridge: Cambridge Univ. Press)
 Weaver, K., Gelbord, J., & Yaqoob, T., 2001, *ApJ*, 550, 261
 Wijnands, R., Miller, J. M., & Lewin, W. H. G., 2001, *IAU Circ.* 7715
 Wilms, J., et al., 2001, *MNRAS*, 328, L27